ADVANCED MATERIALS

www.advmat.de

A Water-Soluble Organic Photocatalyst Discovered for Highly Efficient Additive-Free Visible-Light-Driven Grafting of Polymers from Proteins at Ambient and Aqueous Environments

Yungyeong Lee, Yonghwan Kwon, Youngmu Kim, Changhoon Yu, Siyang Feng, Jeehun Park, Junsang Doh, Reinhold Wannemacher, Byungjin Koo, Johannes Gierschner,* and Min Sang Kwon**

Since the pioneering discovery of a protein bound to poly(ethylene glycol), the utility of protein–polymer conjugates (PPCs) is rapidly expanding to currently emerging applications. Photoinduced energy/electron-transfer reversible addition–fragmentation chain-transfer (PET-RAFT) polymerization is a very promising method to prepare structurally well-defined PPCs, as it eliminates high-cost and time-consuming deoxygenation processes due to its oxygen tolerance. However, the oxygen-tolerance behavior of PET-RAFT polymerization is not well-investigated in aqueous environments, and thereby the preparation of PPCs using PET-RAFT polymerization needs a substantial amount of sacrificial reducing agents or inert-gas purging processes. Herein a novel water-soluble and biocompatible organic photocatalyst (PC) is reported, which enables visible-light-driven additive-free "grafting-from" polymerizations of a protein in ambient and aqueous environments. Interestingly, the developed PC shows unconventional "oxygen-acceleration" behavior for a variety of acrylic and acrylamide monomers in aqueous conditions without any additives, which are apparently distinct from previously reported systems. With such a PC, "grafting-from" polymerizations are successfully performed from protein in ambient buffer conditions under green light-emitting diode (LED) irradiation, which result in various PPCs that have neutral, anionic, cationic, and zwitterionic polyacrylates, and polyacrylamides. It is believed that this PC will be widely employed for a variety of photocatalysis processes in aqueous environments, including the living cell system.

1. Introduction

Post-translational modification of proteins with a synthetic polymer largely influences their properties.[1–3] From a therapeutic point of view, in the case of a protein attached to poly(ethylene glycol) (i.e., PEGylation), stability, bioavailability, and pharmacokinetic/dynamic properties of the protein are enhanced, and immunogenicity is reduced.[4–6] As a result, more than 16 PEGylated protein drugs have received approval from the US Food and Drug Administration (FDA) and have been used clinically worldwide.[7] In addition to conventional PEGylated proteins, protein–polymer conjugates (PPCs) are expected to play an essential role for a variety of emerging applications such as nanomedicine,[8,9] plastics degradation,[10] protein-based membranes/columns for precious metal capture,[11,12] and enzyme catalysis in chemical synthesis via manipulating catalytic activity of enzymes in organic media.[13]

Efficient and site-selective conjugation of a structurally well-defined polymer with

Y. Lee, Y. Kwon, Y. Kim, C. Yu, J. Doh, M. S. Kwon
Department of Materials Science and Engineering
Seoul National University
Seoul 08826, Republic of Korea
E-mail: minsang@snu.ac.kr

Y. Kwon, Y. Kim
Department of Materials Science and Engineering
Ulsan National Institute of Science and Technology (UNIST)
Ulsan 44919, Republic of Korea

The ORCID identification number(s) for the author(s) of this article can be found under https://doi.org/10.1002/adma.202108446.

DOI: 10.1002/adma.202108446

S. Feng, R. Wannemacher, J. Gierschner
Madrid Institute for Advanced Studies
IMDEA Nanoscience, Calle Faraday 9, Campus Cantoblanco, Madrid 28049, Spain
E-mail: johannes.gierschner@imdea.org

J. Park, J. Doh, M. S. Kwon
Research Institute of Advanced Materials
Seoul National University
Seoul 08826, Republic of Korea

B. Koo
Department of Polymer Science and Engineering
Dankook University
Gyeonggi-do 16890, Republic of Korea
E-mail: bkoo@dankook.ac.kr

a narrow molecular weight distribution greatly enhances the preparation efficiency of PPCs, and also reduces the difficulties in purification as well as the unpredictable side effects caused by nonspecifically modified proteins and by-/side products.[6,14] Moreover, this enables precise studies of "structure–property–performance" relationships of PPCs, which accelerate the development of new areas of applications based on PPCs. Therefore, PPCs with a well-defined architecture and high uniformity would be highly beneficial.

Combination of site-selective protein modification and "grafting-from" reversible-deactivation radical polymerization (RDRP) process has been regarded as one of the most promising ways to afford well-defined PPCs with a high uniformity.[6,15] Since the seminal works by the groups of Lewis and Leppard,[16,17] Maynard and co-workers,[18,19] Matyjaszewski and co-workers,[20] precise modification of various proteins with well-defined polymers has been realized by RDRP such as atom-transfer radical polymerization (ATRP) and reversible addition–fragmentation chain-transfer (RAFT) polymerization.[21,22] However, these methods mostly require time-consuming and expensive pre-deoxygenation processes including freeze–pump–thaw and/or inert gas purging that also might cause protein denaturation and/or cell destruction (in the case of in situ preparation of PPCs in living cells).[23–25]

From a merger of RDRP with photochemistry, photomediated RDRP (photo-RDRP) has become even more advantageous in terms of mildness in reaction conditions and versatility of the method.[26–29] Photo-RDRP harnesses visible light as an energy source and thus excludes heat that is used in conventional thermally induced reactions, which prevents denaturation and consequent loss of activity of protein. Particularly, photoinduced electron/energy-transfer-RAFT (PET-RAFT) polymerization does not require a prior deoxygenation process due to its unique feature of "oxygen tolerance,"[30,31] which eliminates the need for external deoxygenation processes for PPCs' syntheses. However, while "oxygen-tolerance" behavior of PET-RAFT polymerization has been well-investigated in organic solvents (i.e., dimethyl sulfoxide (DMSO)), the studies in aqueous environments are still scarce.[32–36] Therefore, the preparation of PPCs by PET-RAFT polymerization requires a substantial amount of sacrificial reducing agents such as tertiary amines and ascorbic acids or an inert gas purging process, which limits the practicability of this method;[37–40] it is noted in this context that PPCs should be prepared in an aqueous environment to prevent the denaturation of a protein. The development of new photocatalysts (PCs) that afford an intrinsically "oxygen-tolerant" photocatalytic system would resolve this problem; however, aqueous PET-RAFT polymerization is substantially limited to several specific PCs such as $Ru(bpy)_3Cl_2$, Eosin Y (and its derivatives), and inorganic PCs that require external additives (previously reported systems on aqueous PET-RAFT are summarized in Figure S1 in the Supporting Information).[37,40–42]

Here, we report a new water-soluble and biocompatible organic PC (i.e., "3DP-MSDP-IPN"; **Figure 1**a), which successfully proceeds visible-light-driven "grafting-from" PET-RAFT polymerizations of a protein at ambient and aqueous environments without additives. To achieve this, water-soluble and weakly electron-donating sulfonate moiety was introduced in one of four donor groups of "4DP-IPN" with a strongly twisted donor–acceptor structure that has been known for highly efficient organic PC for various organic reactions and polymerizations.[43–51] Most excitingly, the discovered PC exhibited unique "oxygen-acceleration" behavior in PET-RAFT polymerizations of a variety of acrylates and acrylamides in both DMSO and aqueous conditions without any additives, which is apparently distinct from previously reported systems.[30,31] Combined experimental and theoretical studies suggested that molecular oxygen acts as an electron shuttle to catalyze the electron transfer between the PC in the excited state and the chain-transfer agent (CTA) (Figure 1d). Here, the PC is expected to play a critical role i) to generate singlet oxygen that is a better oxidant as compared to triplet oxygen and ii) to form superoxide radical anion ($O_2^{\bullet-}$) through electron transfer with singlet and/or triplet oxygen, which is derived from the unique photophysical and electrochemical characteristics of 3DP-MSDP-IPN. With the developed PC, we successfully performed "grafting-from" polymerizations from a protein in ambient buffer conditions under 515 nm green light-emitting diode (LED) irradiation (≈10 mW cm^{-2}), which results in a variety of PPCs having neutral, anionic, cationic, and zwitterionic polyacrylates and polyacrylamides that have rarely been reported before (vide infra). Our water-soluble and biocompatible PC will be applicable to various aqueous photocatalytic and photo-electrocatalytic reactions besides preparation of PPCs.

2. Results and Discussion

2.1. Design Strategy

An ideal PC for visible-light-driven "grafting-from" polymerization of a protein would be a water-soluble and biocompatible molecule exhibiting high catalytic efficiency at ambient and aqueous conditions without any additives that might result in negative consequences for protein functions[52–54] and/or biological systems.[55–57] In particular, intrinsic tolerance of a catalyst system for oxygen is in high demand due to the high-cost, time-consuming, and bio-incompatible pre-deoxygenation processes required.

In order to achieve oxygen tolerance in aqueous PET-RAFT polymerization, the reductive quenching pathway has mostly been used so far, instead of the oxidative quenching pathway (Figure S1, Supporting Information). While the reductive quenching pathway shows great oxygen tolerance, it should require substantial amount of sacrificial reducing agents such as tertiary amines and ascorbic acid;[58,59] according to very recent reports from Boyer's group, "oxygen acceleration," in which oxygen acts as an electron shuttle, could also be attained in organic solvents through the carefully chosen phthalocyanine PCs in the presence of tertiary amines (vide infra).[60] Moreover, the reductive quenching cycle often affords undesired side reactions and less controllability of the polymerization,[40] which originates from the longer lifetime of one-electron-reduced PC ($PC^{\bullet-}$) being an active PC species in a reductive quenching cycle as compared to that of the excited PC species ($^{1/3}PC^*$) being an active PC intermediate in an oxidative quenching cycle.

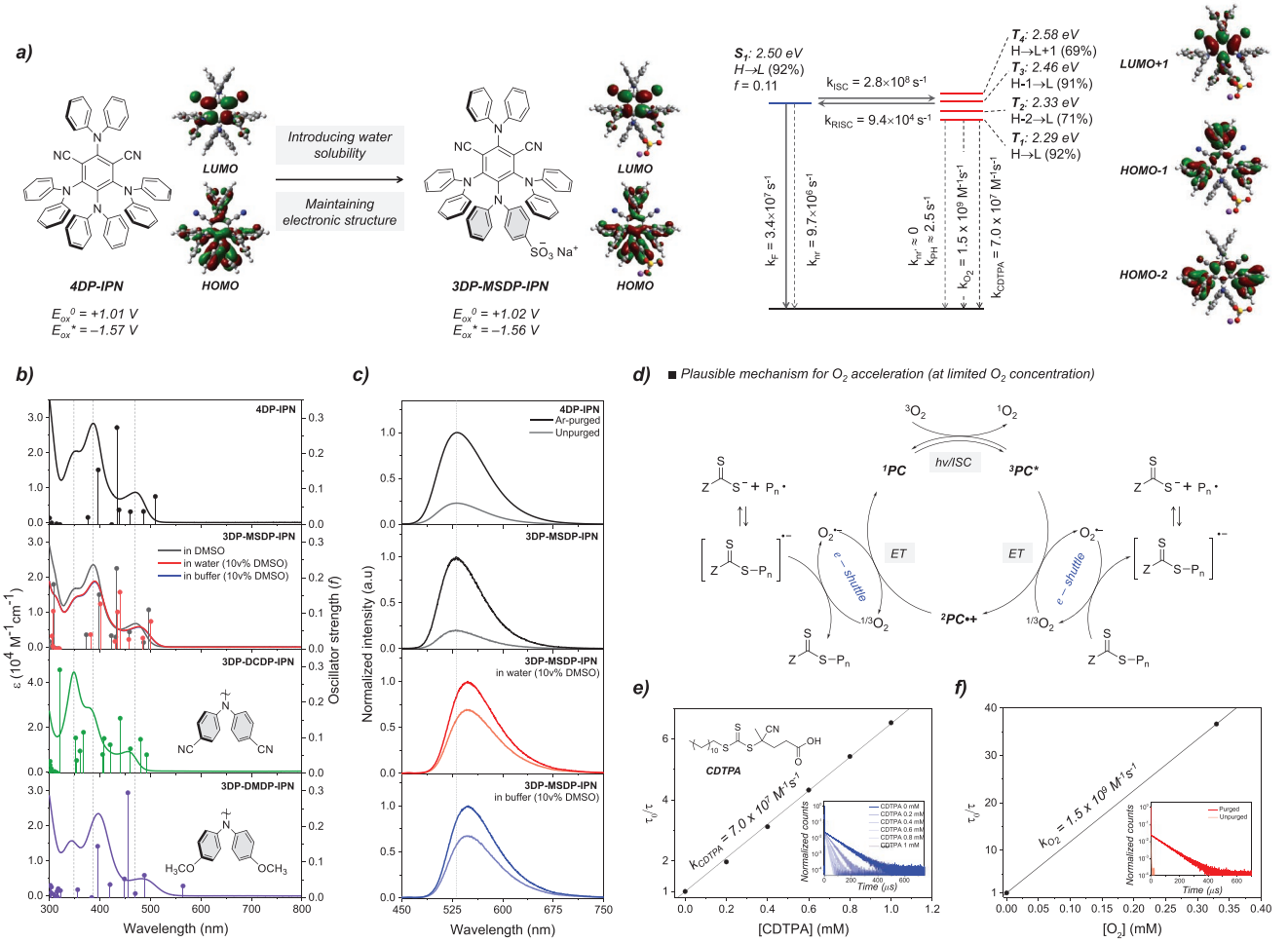

Figure 1. Characterization of 3DP-MSDP-IPN. a) Molecular structure and calculated highest occupied molecular orbital (HOMO) and lowest unoccupied molecular orbital (LUMO) topologies of 4DP-IPN and 3DP-MSDP-IPN with experimentally evaluated E_{ox}^0 and E_{ox}^* values (left). Jablonski diagram of 3DP-MSDP-IPN in DMSO (right). b) UV–vis absorption spectra of 4DP-IPN, 3DP-MSDP-IPN, 3DP-DCDP-IPN, and 3DP-DMDP-IPN each dissolved in the solvent indicated (10×10^{-6} M). The sticks represent oscillator strengths obtained by TD-DFT. c) Photoluminescence (PL) spectra of 4DP-IPN and 3DP-MSDP-IPN in varying solvents (10×10^{-6} M) at room temperature before (dark line) and after (bright line) being degassed with Ar for 10 min. d) Plausible mechanism for PET-RAFT polymerization facilitated by oxygen of limited concentration. e) Stern–Volmer plots for the PL quenching of 3DP-MSDP-IPN in DMSO (10×10^{-6} M) by CDTPA at room temperature. f) Stern–Volmer plots for the PL quenching of 3DP-MSDP-IPN in DMSO (10×10^{-6} M) by oxygen at room temperature (dissolved oxygen concentration in DMSO at room temperature is known to be 0.33×10^{-3} M[69]).

Recently, we reported that cyanoarene-based PC, 4DP-IPN, enabled the oxygen-tolerant PET-RAFT polymerization of methyl methacrylate (MMA) without additives in organic solvent, DMSO (Figure 1a).[45] It has been suggested that a key factor for the excellent oxygen tolerance of this system is the efficient generation of long-lived triplet excited states of the PC. The generated triplet excitons react with molecular oxygen to produce reactive oxygen species (ROS) through a type I and/or type II mechanism, which are subsequently consumed by quencher (here, oxidation of DMSO to dimethyl sulfone), thereby largely decreasing the concentration of dissolved oxygen and consequently furnishing oxygen tolerance (i.e., "pre-deoxygenation" mechanism). Given all these facts, we hypothesized that a water-soluble analog of 4DP-IPN would be a suitable PC candidate for visible-light-driven "grafting-from" polymerization of a protein. Surely, at the beginning, we did not expect "oxygen-tolerance" behavior in aqueous environments without additives, because there are no ROS quenchers in aqueous PET-RAFT polymerization conditions (vide infra).

In order to confer water solubility without perturbing the electronic structures of 4DP-IPN, 3DP-MSDP-IPN was carefully designed, where one of the four donor groups was replaced with sulfonate-substituted diphenylamine while retaining the acceptor moiety (Figure 1a). Sulfonate substitution of diphenylamine was chosen because the sulfonate group is known to be water-soluble, biocompatible, highly stable in aqueous environments, and weakly electron-donating that may not influence the electronic structure;[61–63] in fact, our density functional theory (DFT) calculations show that the highest occupied molecular orbital (HOMO) energy of diphenylamine-4-sulfonate is almost equal to that of diphenylamine (−5.45 and −5.43 eV, respectively; Figure S2, Supporting Information). Full details of the syntheses and characterizations including $^1H(^{13}C)$ NMR and mass spectrometry are shown in Figures S21–S23 (Supporting Information).

2.2. Biocompatibility and Photophysical/Electrochemical Characterizations of 3DP-MSDP-IPN

We first investigated the water solubility of 3DP-MSDP-IPN as compared to that of 4DP-IPN. As expected, 3DP-MSDP-IPN showed greatly enhanced solubility in water in the presence of small amount of DMSO (as low as 1.0 vol%) compared to that of 4DP-IPN (Figure S3, Supporting Information), which is enough for aqueous photocatalysis of interest; since the different amounts of DMSO were used depending on the situation, a vol% of DMSO to the total volume was given where necessary. 3DP-MSDP-IPN was then studied in vitro in cells to evaluate its biocompatibility. 3DP-MSDP-IPN in the absence of light illumination showed no toxicity to HeLa cells up to a concentration of 100×10^{-6} M ($IC_{50} > 200 \times 10^{-6}$ M; Figure S4, Supporting Information) after 48 h of incubation, implying that 3DP-MSDP-IPN could be utilized as a PC for engineering proteins and cell surfaces of living cells[64] as well as for in situ synthesizing polymeric architectures inside living cells.[65]

We then performed photophysical and electrochemical studies, which are the basis for the photocatalytic performance. To perform an accurate comparison with 4DP-IPN, which has very low solubility in water (Figure S3, Supporting Information), photophysical and electrical measurements of 3DP-MSDP-IPN were carried out in DMSO (and CH_3CN). As we anticipated, UV–vis absorption and photoluminescence (PL) spectra and cyclic voltammetry (CV) patterns of 3DP-MSDP-IPN were almost perfectly overlapped with those of 4DP-IPN in DMSO (Figure 1b,c and **Table 1**; Figure S5, Supporting Information). Also, they gave very similar values of PL quantum yields (Φ_F) and prompt and delayed fluorescence lifetimes (τ, Table 1), consequently providing nearly the same excited-state dynamics, i.e., rate constants for radiative and nonradiative singlet state deactivation (k_F, $k_{nr,S}$) and (reverse) intersystem-crossing (k_{ISC}, k_{RISC}).[66] The Jablonski diagrams in Figure 1a (for 3DP-MSDP-IPN) and Figure S6 (Supporting Information) (for 4DP-IPN) sum up the kinetics with the relevant excited-state energies (and compositions), as well as molecular orbital (MO) topologies as calculated by time-dependent (TD) DFT calculations. To validate the effect of substitution, 4,4′-dicyano- and 4,4′-dimethoxydiphenylamine-substituted derivatives of 4DP-IPN (i.e., 3DP-DCDP-IPN and 3DP-DMDP-IPN) were prepared as model compounds. Whereas substitution with diphenylamine-4-sulfonate moiety gave no effect on the overall electronic structure, substitution of diphenylamine with strongly electron-accepting (−CN) and electron-donating ($-OCH_3$) groups resulted in substantial changes in photophysical properties as presented in Figure 1b,c and Table S1 (Supporting Information). More detailed investigations of this aspect are currently underway.

2.3. PET-RAFT Polymerization in DMSO

We next investigated the catalytic performance of 3DP-MSDP-IPN. For a proper comparison, the PET-RAFT polymerization of methyl acrylate (MA) was chosen as a model system. DMSO and 4-cyano-4-[(dodecylsulfanylthiocarbonyl)sulfanyl]-pentanoic acid (CDTPA) were selected as a solvent and CTA, respectively, as they are widely used in PET-RAFT polymerization (**Figure 2**a).[33,45,67] Also, 515 nm green LED was used as an excitation light source. As a negative control, polymerization of MA was conducted in the absence of either a PC or CTA under N_2 or air atmosphere (Figure S7, Supporting Information). These control experiments clearly suggested that the photoiniferter process does not occur under these conditions, and both PC and CTA are essential for the controlled polymerization. Catalytic performance of 4DP-IPN and 3DP-MSDP-IPN was then compared. The polymerizations of MA were successful for both PCs (5 ppm) under N_2 atmosphere and 2 W green LED irradiation (≈1.7 mW cm^{-2}) conditions (Figure S7, Supporting Information). As hypothesized, the results were very similar in terms of conversion and controllability, confirming that the catalytic performance in DMSO of 3DP-MSDP-IPN is comparable to that of 4DP-IPN.

We then tested the oxygen tolerance of 3DP-MSDP-IPN for the PET-RAFT polymerization of MA in DMSO with and without N_2 purging. Very surprisingly, the polymerization of

Table 1. Photophysical and electrochemical properties of 4DP-IPN and 3DP-MSDP-IPN in varying solvents. Ground-state redox potentials were measured in CH_3CN (0.2×10^{-3}M) versus Ag/AgCl. E_{00} was evaluated from onset of gated PL spectrum at room temperature. Excited-state redox potentials were calculated from the Rehm–Weller equation ($E_{ox/red}^{*} = -E_{00} + E_{ox/red}^{0}$).

PC	Solvent	$\lambda_{max,abs}$ [nm]	$\lambda_{max,em}$ [nm]	E_{red}^{0} [V]	E_{ox}^{0} [V]	E_{00} [eV]	E_{red}^{*} [V]	E_{ox}^{*} [V]	Atmosphere	ϕ_F [%]	τ_{prompt} [ns]	$\tau_{delayed}$ [µs]
4DP-IPN	DMSO	471	536	–1.66	+1.01	2.58	0.92	–1.57	N_2	85	3.3	82
									Air	14	3.2	4.0
3DP-MSDP-IPN	DMSO	470	536	–1.60	+1.02	2.58	0.98	–1.56	N_2	78	3.1	79
									Air	13	3.1	2.9
	Water (10 vol% DMSO)	476	554	–1.60	+1.02	2.50	0.90	–1.48	N_2	9	2.2	21
									Air	7	2.2	2.5
	Buffer (10 vol% DMSO)	476	547	–1.60	+1.02	2.50	0.90	–1.48	N_2	9	2.1	20.2
									Air	7	2.1	3.0

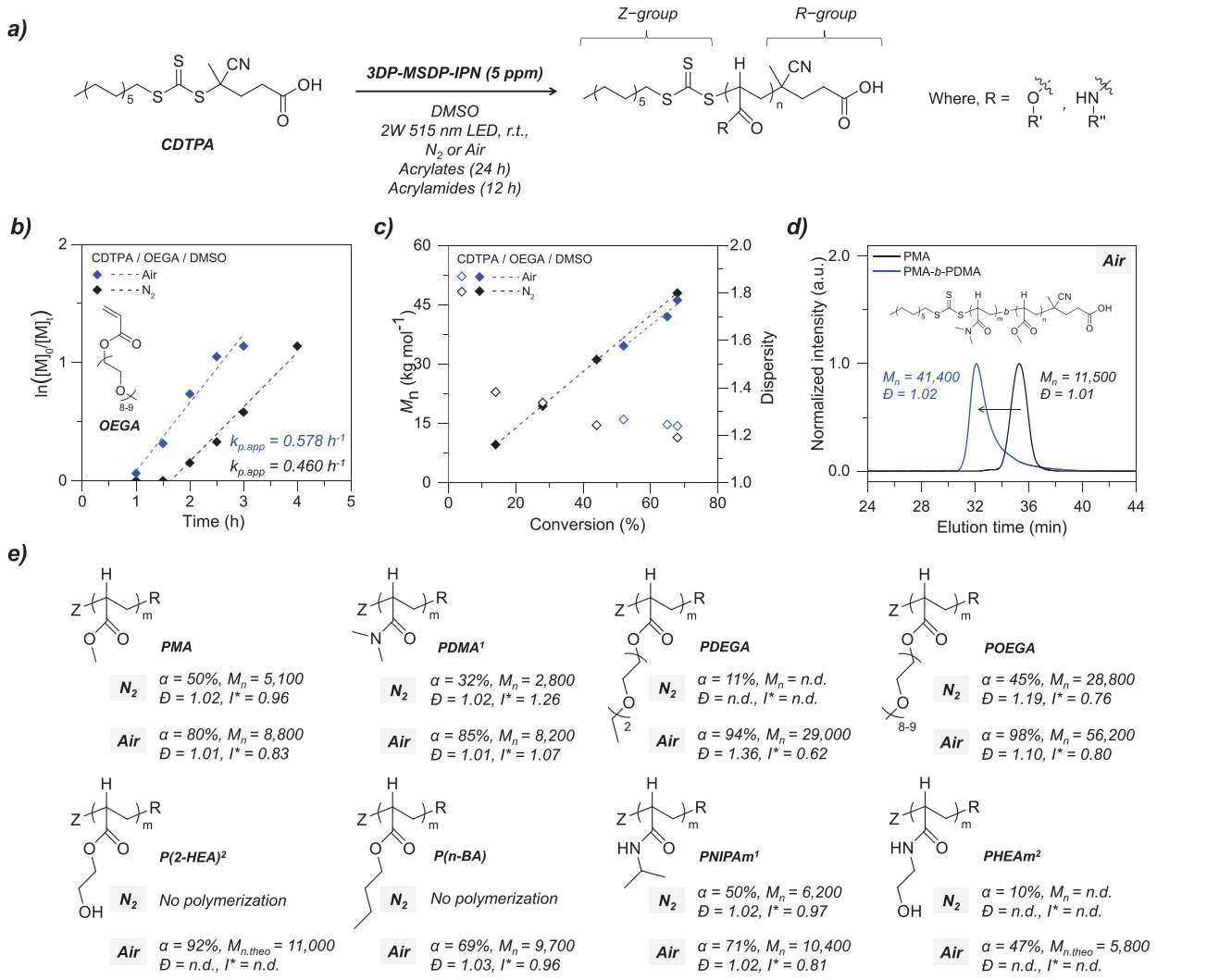

Figure 2. Results of PET-RAFT polymerizations in DMSO. a) Reaction scheme of PET-RAFT polymerization using CDTPA as CTA. b) Kinetic plots for PET-RAFT polymerization of OEGA under air and N_2 using 3DP-MSDP-IPN (5 ppm): $\ln([M]_0/[M]_t)$ versus reaction time. c) M_n (filled) and dispersity (empty) versus conversion. d) GPC traces of poly(methyl acrylate) (PMA, black) and poly(methyl acrylate)-*b*-poly(*N*,*N*-dimethyl acrylamide) (PMA-*b*-PDMA, blue). e) Summary of polymers prepared from various acrylate and acrylamide monomers. 1) The reaction was conducted for 3 h (PDMA) or 4 h (PNIPAm) instead of 12 h to clearly observe the "oxygen-acceleration" behavior; 2) the polymers could not be analyzed by GPC in tetrahydrofuran (THF) due to insolubility and in water due to incompatibility of the polymers containing residual DMSO.

MA gave substantially higher conversion ($\alpha = 80\%$) in the presence of oxygen (without N_2 purging) than after purging with N_2 (α = 50%) while maintaining the excellent controllability (Figure 2e). Such "oxygen-acceleration" behavior was observed indeed in Boyer's group as stated above, however, in a reductive quenching cycle in the presence of sacrificial reducing agents.[60] This rather counterintuitive "oxygen-acceleration" behavior was similarly observed for a variety of acrylate and acrylamide monomers (Figure 2e). To understand the origin of this phenomenon, kinetics of PET-RAFT polymerizations of oligo(ethylene glycol) methyl ether acrylate (OEGA) were monitored by ^{1}H NMR and gel-permeation chromatography (GPC) for 3DP-MSDP-IPN (5 ppm) under air and N_2 atmosphere (Figure 2b,c; Figure S8, Supporting Information); here, OEGA was chosen as a model system of the kinetics studies for the comparison to PET-RAFT polymerizations in aqueous environment. A linear relation of conversion versus time, and of M_n versus conversion, was observed for both cases, suggesting the living characters of these polymerizations being also supported by successful synthesis of block copolymer (Figure 2d). Good temporal control in polymerization was observed in a light "ON"/"OFF" experiment (Figure S9, Supporting Information). Moreover, the apparent rate of propagation ($k_{p,app}$) and inhibition period were evaluated from kinetic plots (Figure 2b). Obvious increase in $k_{p,app}$ (from 0.460 to 0.578 h^{-1}) and decrease in inhibition period (from 98 to 57 min) were found for the polymerization under air, suggesting that the activation step in PET-RAFT polymerization (i.e., electron transfer from PC in the excited states ($^{1/3}PC^*$) to dormant species) could be facilitated in the presence of oxygen. In other words, oxygen might

catalyze the electron-transfer process between $^{1/3}PC^*$ and dormant species (Figure 1d), which rather contradicts the previously proposed mechanism of "oxygen tolerance" (vide supra, i.e., "pre-deoxygenation mechanism").

In order to clarify the role of oxygen in "oxygen-acceleration" behavior, we performed PL quenching studies in the presence of CDTPA and oxygen (Figure 1e,f). In the quenching experiments, no lifetime changes were observed in the prompt PL, but very significant changes were observed in the delayed PL; see Figure 1e,f and Table 1; this clearly evidences that the long-lived lowest triplet excited state (T_1) is mainly affected by quenching. This can be directly seen in the evaluated kinetic constants related to excited-state dynamics and electron-transfer kinetics (Figure 1a, vide infra). In fact, quenching constants were evaluated to be $\approx 7.0 \times 10^7$ M^{-1} s^{-1} (for CDTPA) and $\approx 1.5 \times 10^9$ M^{-1} s^{-1} (for oxygen) by Stern–Volmer analysis;[68,69] it is noted that the quenching constant for oxygen is very fast, reaching the diffusion limit in DMSO ($\approx 3 \times 10^9$ M^{-1} s^{-1}, as obtained from the Stokes–Einstein equation).[70] Given the concentration of CDTPA and oxygen in the polymerization conditions (11.3×10^{-3} and 0.67×10^{-3} M, respectively; here, dissolved oxygen concentration was calculated for the mixed solutions of DMSO and monomers with a 1:1 volume ratio), the rate of electron/energy transfer between $^3PC^*$ and oxygen is calculated to be $\approx 1.0 \times 10^6$ s^{-1}, which is faster than that between $^3PC^*$ and CDTPA ($\approx 7.9 \times 10^5$ s^{-1}), implying that direct electron transfer from $^3PC^*$ to CDTPA (and/or dormant species) might not be favored in the presence of oxygen. Very recently, Boyer and co-workers proposed the oxygen-mediated reductive quenching pathway (O-RQP) as a new mechanism to rationalize the "oxygen-acceleration" behavior observed for carefully chosen PCs in the presence of triethylamine (TEA) as a sacrificial reducing agent,[60] where the author demonstrated the thermodynamic feasibility of O-RQP through quantum-chemical (QC) calculations and studies of structure–property–performance relationships. Here, oxygen acts as an electron shuttle to catalyze the electron transfer between TEA and CTA (and/or dormant species) in the overall reductive quenching cycle. The role of PC is rather limited to be a singlet oxygen generator. All those things considered; we propose the "oxygen-acceleration" mechanism, as presented in Figure 1d. While oxygen acts as an electron shuttle between $^{1/3}PC^*$ and CTA as in the O-RQP, the PC plays a more essential role: i) as a generator of singlet oxygen, which is far stronger oxidant than triplet oxygen and ii) as a photoreductant to form the superoxide radical ion ($O_2^{\bullet -}$), which originates from the photophysical and electrochemical features of 3DP-MSDP-IPN—i) ultraefficient generation of long-lived triplet excited states (according to our simulations, triplet concentration in photostationary state of 3DP-MSDP-IPN is ≈2 orders of magnitude higher than that of $Ir(ppy)_3$ and $Ru(bpy)_3^{2+}$; see Figure S10 in the Supporting Information), ii) substantially negative excited-state oxidation potential ($E_{ox}^* = -1.56$ V), and iii) highly stable radical cation as evidenced by reversible waves in CV. Given the singlet–triplet energy gap and reduction potential of molecular oxygen ($\Delta E_{ST} \approx 0.98$ eV and $E_{red}^0 \approx -0.60$–1.00 V vs saturated calomel electrode (SCE)),[71–74] overall processes following the proposed mechanism are thermodynamically feasible. The half-life and diffusion length of $O_2^{\bullet -}$, which is known to be rather long (≈1 µs and 1 µm (in water), respectively),[74,75] also support our proposed mechanism. Nevertheless, more in-depth studies are currently on-going in our laboratory.

2.4. PET-RAFT Polymerization in Water

We then expanded our studies to aqueous PET-RAFT polymerizations. Here, 4-((((2-Carboxyethyl)thio)carbonothioyl)thio)-4-cyanopentanoic acid (CETCPA) was used as a CTA instead of CDTPA due to its excellent water solubility (**Figure 3**). For the comparison of PET-RAFT polymerization in DMSO, OEGA was selected as a monomer. Apart from the change in solvent, all other conditions were exactly the same as those in the DMSO experiment. As a negative control, the polymerization of OEGA was performed in the absence of PC or CTA, providing no polymers, as we expected (Figure S11, Supporting Information). Interestingly, no polymerization took place in inert atmosphere, while 98% conversion was obtained in air with an excellent control ($Đ = 1.10$, $I^* = 0.83$), implying that the "oxygen-acceleration" effect is more pronounced in aqueous conditions. As shown in Figure 3e, similar behaviors were found in a variety of water-soluble acrylates and acrylamides. It may be noted that the catalytic performance of the PC developed here exceeded, without any additives, that of the previously reported water-soluble PCs including $Ru(bpy)_3Cl_2$ and Eosin Y disodium salt in the presence of additives (Figure S12, Supporting Information).

Kinetics of the aqueous PET-RAFT polymerization of OEGA was monitored under air to investigate the "oxygen-acceleration" effect as well as the livingness of the polymerization. Again, no polymerization was seen in the kinetics monitoring under N_2 atmosphere (Figure 3b,c; Figure S13, Supporting Information). A clear linear relationship of conversion versus time, and of M_n versus conversion, was found, indicating the livingness of the polymerization, which is also supported by the fact that the synthesis of a block copolymer was successful (Figure 3d). Polymerization was observed only when light is turned on, reflecting good temporal control (Figure S14, Supporting Information). From the kinetics plot, $k_{p,app}$ was calculated to be 0.167 h^{-1}, which is smaller than that in DMSO conditions.

In order to further understand the pronounced "oxygen-acceleration" behavior and rate retardation in aqueous conditions, photophysical properties of the aqueous solution of 3DP-MSDP-IPN were studied (Figure 1b,c and Table 1). The absorption and emission spectra in water show a small but distinct bathochromic shift (0.04 eV) versus that in DMSO. According to the TD-DFT calculations, this is not due to a polarizability effect, but is ascribed to dissociation of the sodium ion in water (Figure 1b; Figure S6, Supporting Information). Strikingly, the overall Φ_F decreases from 78% in DMSO to 9% in water under N_2 purged conditions, despite careful deaeration by applying a repeated freeze–pump–thaw procedure. According to our kinetic analysis (Figure S6, Supporting Information), this is mainly ascribed to a strong increase of nonradiative deactivation for the S_1 state ($k_{nr,S}$; see Figure 1a and also Figure S6 in the Supporting Information), while the other rates are very similar to DMSO. In fact, $k_{nr,S}$ in solution combines internal conversion (IC) and vibrational relaxation (VR). While PL quenching in water is sometimes ascribed to high-energy vibrations, which slows down VR,[76] the very pronounced

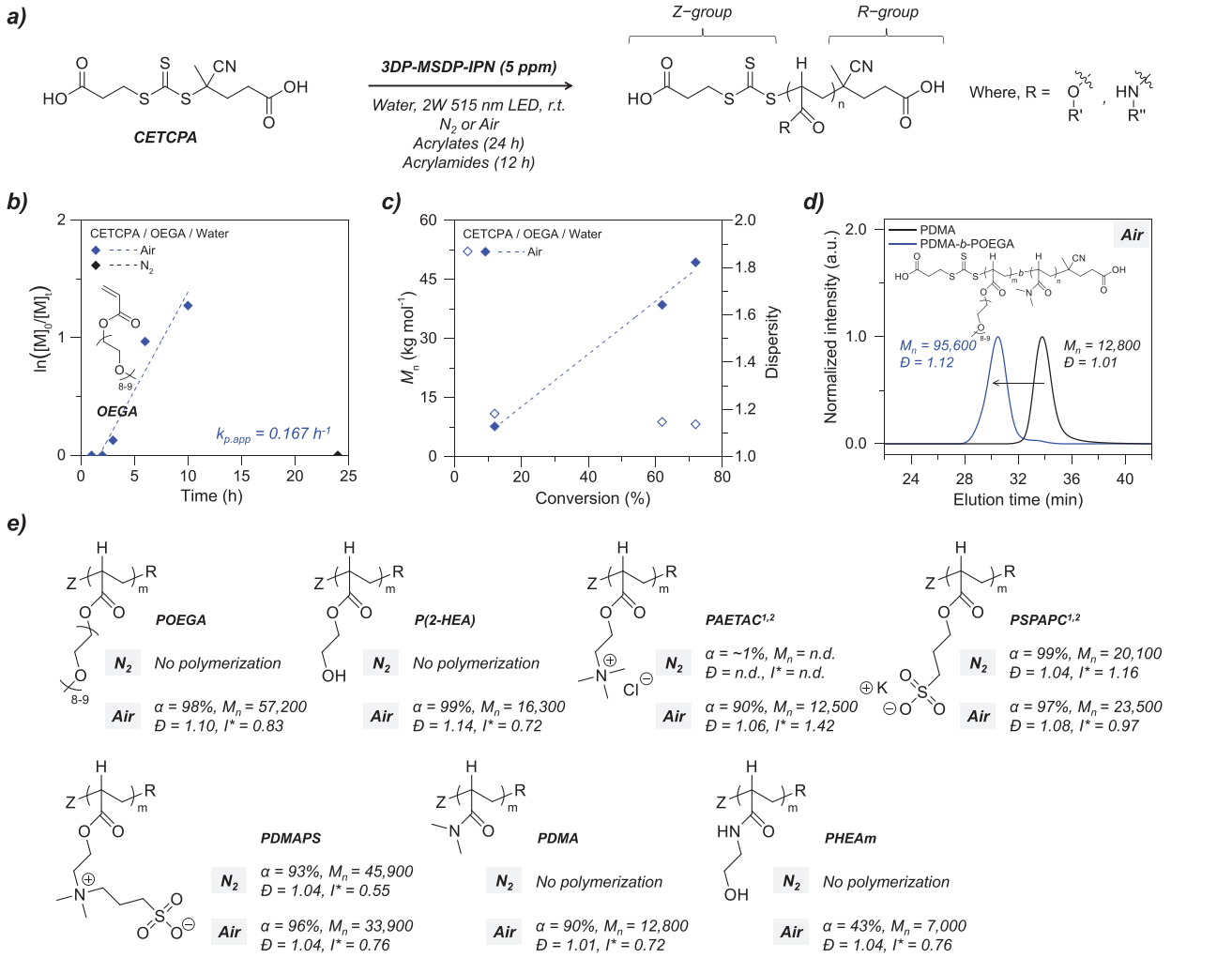

Figure 3. Results of PET-RAFT polymerizations in water. a) Reaction scheme of PET-RAFT polymerization using CETCPA as CTA. b) Kinetic plots for PET-RAFT polymerization of OEGA under air and N_2 using 3DP-MSDP-IPN (5 ppm): $\ln([M]_0/[M]_t)$ versus reaction time. c) M_n (filled) and dispersity (empty) versus conversion. d) GPC traces of poly(*N*,*N*-dimethyl acrylamide) (PDMA, black) and poly(*N*,*N*-dimethyl acrylamide)-*b*-poly(oligo(ethylene glycol) methyl ether acrylate) (PDMA-*b*-POEGA, blue). e) Summary of polymers prepared from various acrylate and acrylamide monomers. 1) The reaction was conducted for 1.5 h (PAETAC) instead of 24 h to clearly observe the "oxygen-acceleration" behavior. In case of PSPAPC, the higher catalyst loading of 50 ppm was used for reproducibility; 2) the GPC analysis was done using an refractive index (RI) detector instead of MALLS.

increase of $k_{nr,S}$ may rather suggest an enhanced IC process, possibly by the formation of specific hydrogen bonds with the surrounding water molecules.[77] The increase in $k_{nr,S}$ affects the delayed emission much more than the prompt one, as seen in the significant decrease in $\tau_{delayed}$ from ≈80 µs in DMSO to ≈20 µs in water; see Table 1. Under air atmosphere, the delayed component shortens to ≈3 µs, which is evidently sufficient to maintain the photocatalytic activity, however, retarding the reaction rate.

Given all experiments and theoretical calculations presented so far, the mechanistic origin of "oxygen-acceleration" behavior in water and DMSO is expected to be the same. Thus, the pronounced effect in aqueous environments seems to be due to the differences in singlet oxygen quenching ability between water and DMSO. However, DMSO is known as a good singlet oxygen quencher, and water does not act as a quencher.[34,60,67] Therefore, substantial oxygen consumption takes place in DMSO as compared to water, which reduces the catalytic role of oxygen and, hence, the "oxygen-acceleration" behavior. For poly(3-sulfopropyl acrylate potassium salt) (PSPAPC) and poly(3-[[2-(acryloyloxy)ethyl]dimethylammonio]propane-1-sulfonate) (PDMAPS) (Figure 3e), the reaction time was too long to observe the behavior and, thereby, more investigations are planned for this interesting "oxygen-acceleration" behavior.

2.5. "Grafting-From" PET-RAFT Polymerization from BSA

We finally conducted "grafting-from" PET-RAFT polymerization of a protein. Bovine serum albumin (BSA) was selected, as a model protein since modification of a free thiol at the Cys-34 residue of BSA is well established.[18,19,37,78] Following

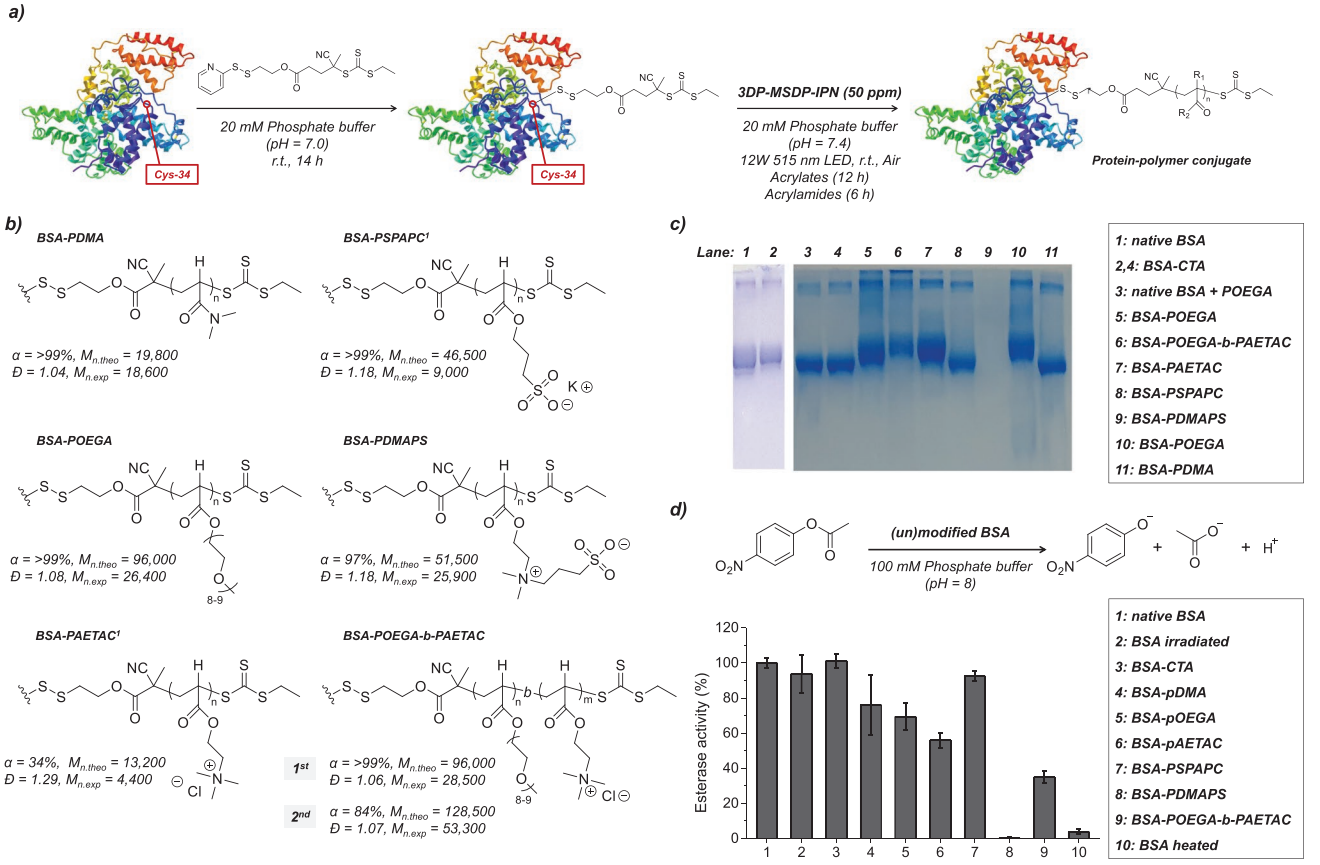

Figure 4. Results of "grafting-from" PET-RAFT polymerization from BSA. a) Reaction scheme of synthesis of BSA–macroinitiator and "grafting-from" PET-RAFT polymerization thereafter. b) Summary of grafted polymers prepared from various acrylate and acrylamide monomers. c) SDS-PAGE analysis of native BSA, BSA–macroinitiator, and various BSA–polymer conjugates. d) Esterase activity of BSA (and its derivatives) and various BSA–polymer conjugates.1) The GPC analysis was done using an RI detector instead of MALLS. In case of PSPAPC, the higher catalyst loading of 500 ppm was used.

the previous reports,[79] a trithiocarbonate-based CTA (4-cyano-4-(((ethylthio)carbonothioyl)thio)pentanoic acid, CETPA) with a pyridyl disulfide moiety (P-CETPA) was prepared (**Figure 4**a). The conjugation of P-CETPA to BSA was carried out in 20×10^{-3} M phosphate buffer (pH = 7.0) with an excess amount of P-CETPA at ambient conditions. After 14 h, the mixture solution was then purified to remove excess P-CETPA by dialysis against water followed by freeze-drying to afford BSA–macroinitiator in powder form. Matrix-assisted laser desorption ionization time-of-flight (MALDI-TOF) analysis further confirmed the successful formation of the BSA–macroinitiator (Figure S15, Supporting Information).

We first tried to perform PET-RAFT polymerization from BSA–macroinitiator in ambient buffer environments. Here, we used *N*,*N*-dimethylacrylamide (DMA) as a model monomer for the "grafting-from" preparation of PPCs due to its simplicity and wide utility. In order to prevent protein denaturation, polymerization conditions were optimized (with DMA) in more diluted conditions and reduced reaction time with higher PC loadings (50 ppm) and higher light intensity (12 W green LED irradiation (≈10 mW cm^{-2}); see Figure 4a and also Figure S16 in the Supporting Information). Polymerizations of the other acrylate and acrylamide monomers were then conducted in the same conditions. Conjugation of a polymer to a BSA–macroinitiator was characterized by ^{1}H-NMR, GPC–multi-angle laser light scattering (MALLS), and sodium dodecyl sulfate-poly(acrylamide) gel electrophoresis (SDS-PAGE) analyses of the reaction aliquot (Figure 4b–d).

Most monomers gave a quantitative conversion confirmed by ^{1}H-NMR, but not all conjugates showed a clear shift in GPC traces presumably due to the limited solubility of the resulting protein–polymer conjugates in eluent of our GPC system (Figure S17, Supporting Information). We assume that the appearance of a substantially wide range of monomers with different characteristics complicates the analysis of their resulting protein conjugates. For example, the successful conjugation of DMAPS polymers (PDMAPS) could be clearly observed both in NMR and aqueous GPC, albeit not in SDS-PAGE (no trace was seen) (Figure 4c; Figure S17, Supporting Information). Addition of an excess amount of tris(2-carboxyethyl)phosphine hydrochloride (TCEP) to the resulting PPCs provided polymers with a narrow dispersity, cleaved from the protein, which further validates that the polymerization proceeded in a controlled manner. To summarize, as listed in Figure 4b, the polymerizations of a variety of water-soluble monomers having neutral, anionic, cationic, and zwitterionic acrylates/acrylamides gave successful syntheses of PPCs. Notably, poly(oligo(ethylene glycol) methyl ether acrylate)-poly([2-(acryloyloxy)ethyl]trimethylammonium chloride) (POEGA–PAETAC) block copolymer was also successfully prepared from the BSA–macroinitiator

with a continuous monomer feeding process at ambient conditions, which has not been demonstrated before.

However, the molecular weight of the grown polymers from the protein was shown to be smaller as compared to the theoretical molecular weight calculated from the conversion, which has not been observed in the PET-RAFT polymerizations in the absence of protein (Figure 4b, vide supra). This phenomenon was seen for the most of monomers (the only exception here was DMA), implying that additional initiation sites might exist in our experimental conditions. In order to understand this behavior, a series of negative control experiments was conducted with OEGA (Figure S19, Supporting Information). Surprisingly, the use of native BSA instead of BSA–macroinitiator resulted in the formation of "hydrogel." Considering the structural feature of BSA that there are 17 disulfide bonds,[80] disulfide bonds might generate thiyl radicals by PC-mediated energy/electron-transfer reactions[81] followed by thiyl-radical-mediated polymerizations and thereby, network formation; it is here noted that native BSA gave negligible polymerization in the absence of PC, indicating that PC plays an essential role for native BSA-initiated gelation. However, the reaction for thiyl radical formation might be far slower than the radical generation from a trithiocarbonate moiety, which is supported by the fact that BSA–macroinitiator provided the successful syntheses of PPCs. In particular, for a monomer with a high rate of propagation (i.e., DMA), the molecular weight obtained from GPC–MALLS is in well accordance to a theoretical molecular weight, further confirming our argument; it is presumed that a substantial amount of DMA monomers was consumed before the activation of disulfide bonds.

The effect of a variety of polymers on the enzymatic activity of BSA was then studied (Figure 4d). BSA is known to show an esterase-like activity, which can be evaluated from the hydrolysis experiments of *p*-nitrophenyl acetate where the absorbance at 405 nm of the hydrolyzed product, *p*-nitrophenol, was measured. Native BSA with or without irradiation and BSA–macroinitiator retained the esterase-like activity in contrast to BSA heated at 80 °C for 5 h, indicating that the polymerization condition does not cause protein denaturation. The synthesized PPCs with a variety of polymers showed activity in varying degrees, clearly indicating that the enzymatic activity could be tailored by the structure of polymers conjugated to the protein. Although the modification with the grown polymers lowered the activity in some cases, BSA–PSPAPC conjugates indicated the similar BSA activity to the native BSA with an additional benefit of tuning the surface changes of BSA, which is often hard to achieve by chemistries with small molecules. Moreover, interestingly, almost no activity was retained for BSA–PDMAPS conjugates, which might enable "activity-switching behavior" of the enzyme by introducing external stimuli–responsive moiety into the polymers. The related researches are currently underway.

3. Conclusion

A highly efficient water-soluble and biocompatible organic PC was discovered, which enables the syntheses of well-defined PPCs through a "grafting-from" PET-RAFT polymerization at ambient/aqueous conditions without additives. Incorporation of water-soluble and weakly electron-donating sulfonate moiety into one of four donor groups of the well-known highly efficient organic PC, 4DP-IPN, yields 3DP-MSDP-IPN with the same electronic structure, but, largely enhanced water solubility. Unconventional "oxygen-acceleration" behavior was observed for the PET-RAFT polymerization of acrylic and acrylamide monomers in the presence of 3DP-MSDP-IPN in which oxygen acts as an electron shuttle between $^3PC^*$ and CTA. Here, the PC plays an important role: i) singlet oxygen generator and ii) photoreductant to form superoxide radical ion ($O_2^{\bullet-}$), which originates from the photophysical and electrochemical features of 3DP-MSDP-IPN. With 50 ppm of 3DP-MSDP-IPN, we successfully performed "grafting-from" polymerizations from BSA in biorelevant conditions under green LED irradiation, which allows for preparation of various types of PPCs with neutral, anionic, cationic, and zwitterionic polyacrylates and polyacrylamides. We believe that our PC system will be actively utilized for a variety of photocatalysis processes in aqueous environments including the living cell system.

Supporting Information

Supporting Information is available from the Wiley Online Library or from the author.

Acknowledgements

This work was supported by Creative-Pioneering Researchers Program through Seoul National University (0417-20200126) and by the Basic Science Research Program through the National Research Foundation of Korea (NRF), which was funded by the Ministry of Education (2019R1I1A2A01059288) and the Ministry of Science and ICT (MSIT) (2021R1A5A1030054). The work at IMDEA was supported by the Spanish Ministry for Science (MINECO/MICINN–FEDER projects CTQ2017–87054, and RTI2018-097508-B-I00) by the "Severo Ochoa" programme for Centers of Excellence in Research and Development (MINECO; grant SEV-2016-0686 and MICINN CEX2020-001039-S), European Union structural funds and Comunidad de Madrid NMAT2D-CM Program (P2018/NMT-4511), and Campus of International Excellence UAM + CSIC.

Conflict of Interest

The authors declare no conflict of interest.

Data Availability Statement

The data that support the findings of this study are available from the corresponding author upon reasonable request.

Keywords

organic photocatalysts, photocatalyzed RAFT, photoredox catalysis, protein–polymer conjugates, reversible-deactivation radical polymerization

Received: October 21, 2021
Revised: January 11, 2022
Published online: February 23, 2022

[1] J. Y. Shu, B. Panganiban, T. Xu, *Annu. Rev. Phys. Chem.* **2013**, *64*, 631.
[2] I. Cobo, M. Li, B. S. Sumerlin, S. Perrier, *Nat. Mater.* **2015**, *14*, 143.
[3] T. A. Wright, R. C. Page, D. Konkolewicz, *Polym. Chem.* **2019**, *10*, 434.
[4] A. Abuchowski, T. van Es, N. C. Palczuk, F. F. Davis, *J. Biol. Chem.* **1977**, *252*, 3578.
[5] J. M. Harris, R. B. Chess, *Nat. Rev. Drug Discovery* **2003**, *2*, 214.
[6] E. M. Pelegri-O'Day, E.-W. Lin, H. D. Maynard, *J. Am. Chem. Soc.* **2014**, *136*, 14323.
[7] I. Ekladious, Y. L. Colson, M. W. Grinstaff, *Nat. Rev. Drug Discovery* **2019**, *18*, 273.
[8] C. A. Stevens, K. Kaur, H.-A. Klok, *Adv. Drug Delivery Rev.* **2009**, *61*, 1203.
[9] A. Grigoletto, T. Tedeschini, E. Canato, G. Pasut, *WIREs Nanomed. Nanobiotechnol.* **2021**, *13*, e1689.
[10] C. DelRe, Y. Jiang, P. Kang, J. Kwon, A. Hall, I. Jayapurna, Z. Ruan, L. Ma, K. Zolkin, T. Li, C. D. Scown, R. O. Ritchie, T. P. Russell, T. Xu, *Nature* **2021**, *592*, 558.
[11] W.-H. Leung, P.-K. So, W.-T. Wong, W.-H. Loa, P.-H. Chan, *RSC Adv.* **2016**, *6*, 106837.
[12] M. Liu, L. Jia, Z. Zhao, Y. Han, Y. Li, Q. Peng, Q. Zhang, *Chem. Eng. J.* **2020**, *390*, 124667.
[13] J. Zhu, Y. Zhang, D. Lu, R. N. Zare, J. Ge, Z. Liu, *Chem. Commun.* **2013**, *49*, 6090.
[14] J. C. M. van Hest, *Polym. Rev.* **2007**, *47*, 63.
[15] B. S. Sumerlin, *ACS Macro Lett.* **2012**, *1*, 141.
[16] A. L. Lewis, S. W. Leppard, *US 8053520*, **2011**.
[17] A. L. Lewis, *US 8431113*, **2013**.
[18] D. Bontempo, K. L. Heredia, B. A. Fish, H. D. Maynard, *J. Am. Chem. Soc.* **2004**, *126*, 15372.
[19] K. L. Heredia, D. Bontempo, T. Ly, J. T. Byers, S. Halstenberg, H. D. Maynard, *J. Am. Chem. Soc.* **2005**, *127*, 16955.
[20] B. S. Lele, H. Murata, K. Matyjaszewski, A. J. Russell, *Biomacromolecules* **2005**, *6*, 3380.
[21] E. M. Pelegri-O'Day, H. D. Maynard, *Acc. Chem. Res.* **2016**, *49*, 1777.
[22] M. S. Messina, K. M. M. Messina, A. Bhattacharya, H. R. Montgomery, H. D. Maynard, *Prog. Polym. Sci.* **2020**, *100*, 101186.
[23] L. Zhao, L. Li, G. Liu, L. Chen, X. Liu, J. Zhu, B. Li, *Food Res. Int.* **2013**, *53*, 409.
[24] L. Zhang, Y. Zhang, J. Cheng, L. Wang, X. Wang, M. Zhang, Y. Gao, J. Hu, X. Zhang, J. L. Lü, G. Li, R. Tai, H. Fang, *Sci. Rep.* **2017**, *7*, 10176.
[25] K. A. Pikal-Cleland, N. Rodríguez-Hornedo, G. L. Amidon, J. F. Carpenter, *Arch. Biochem. Biophys.* **2000**, *384*, 398.
[26] M. Chen, M. Zhong, J. A. Johnson, *Chem. Rev.* **2016**, *116*, 10167.
[27] N. Corrigan, S. Shanmugam, J. Xu, C. Boyer, *Chem. Soc. Rev.* **2016**, *45*, 6165.
[28] X. Pan, M. A. Tasdelen, J. Laun, T. Junkers, Y. Yagci, K. Matyjaszewski, *Prog. Polym. Sci.* **2016**, *62*, 73.
[29] Y. Lee, C. Boyer, M. S. Kwon, *Nat. Rev. Mater.* **2022**, *7*, 74.
[30] J. Yeo, R. Chapman, A. J. Gormley, C. Boyer, *Chem. Soc. Rev.* **2018**, *47*, 4357.
[31] M. D. Nothling, Q. Fu, A. Reyhani, S. Allison-Logan, K. Jung, J. Zhu, M. Kamigaito, C. Boyer, G. G. Qiao, *Adv. Sci.* **2020**, *7*, 2001656.
[32] J. Xu, K. Jung, C. Boyer, *Macromolecules* **2014**, *47*, 4217.
[33] S. Shanmugam, J. Xu, C. Boyer, *J. Am. Chem. Soc.* **2015**, *137*, 9174.
[34] N. Corrigan, D. Rosli, J. W. J. Jones, J. Xu, C. Boyer, *Macromolecules* **2016**, *49*, 6779.
[35] C. Wu, S. Shanmugam, J. Xu, J. Zhu, C. Boyer, *Chem. Commun.* **2017**, *53*, 12560.
[36] C. Wu, N. Corrigan, C.-H. Lim, K. Jung, J. Zhu, G. Miyake, J. Xu, C. Boyer, *Macromolecules* **2019**, *52*, 236.
[37] J. Xu, K. Jung, N. A. Corrigan, C. Boyer, *Chem. Sci.* **2014**, *5*, 3568.
[38] B. S. Tucker, M. L. Coughlin, C. A. Figg, B. S. Sumerlin, *ACS Macro Lett.* **2017**, *6*, 452.
[39] C. Fu, B. Demir, S. Alcantara, V. Kumar, F. Han, H. G. Kelly, X. Tan, Y. Yu, W. Xu, J. Zhao, C. Zhang, H. Peng, C. Boyer, T. M. Woodruff, S. J. Kent, D. J. Searles, A. K. Whittaker, *Angew. Chem., Int. Ed.* **2020**, *59*, 4729.
[40] R. A. Olson, J. S. Levi, G. M. Scheutz, J. J. Lessard, C. A. Figg, M. N. Kamat, K. B. Basso, B. S. Sumerlin, *Macromolecules* **2021**, *54*, 4880.
[41] J. Xu, S. Shanmugam, H. T. Duonga, C. Boyer, *Polym. Chem.* **2015**, *6*, 5615.
[42] S. Allison-Logan, Q. Fu, Y. Sun, M. Liu, J. Xie, J. Tang, G. G. Qiao, *Angew. Chem., Int. Ed.* **2020**, *59*, 21392.
[43] V. K. Singh, C. Yu, S. Badgujar, Y. Kim, Y. Kwon, D. Kim, J. Lee, T. Akhter, G. Thangavel, L. S. Park, J. Lee, P. C. Nandajan, R. Wannemacher, B. Milián-Medina, L. Lüer, K. S. Kim, J. Gierschner, M. S. Kwon, *Nat. Catal.* **2018**, *1*, 794.
[44] M. Garreau, F. L. Vaillant, J. Waser, *Angew. Chem., Int. Ed.* **2019**, *58*, 8182.
[45] Y. Song, Y. Kim, Y. Noh, V. K. Singh, S. K. Behera, A. Abudulimu, K. Chung, R. Wannemacher, J. Gierschner, L. Lüer, M. S. Kwon, *Macromolecules* **2019**, *52*, 5538.
[46] J.-H. Back, Y. Kwon, J. C. Roldao, Y. Yu, H.-J. Kim, J. Gierschner, W. Lee, M. S. Kwon, *Green Chem.* **2020**, *22*, 8289.
[47] J.-H. Back, Y. Kwon, H.-J. Kim, Y. Yu, W. Lee, M. S. Kwon, *Molecules* **2021**, *26*, 385.
[48] Y. Lee, M. S. Kwon, *Eur. J. Org. Chem.* **2020**, *38*, 6028.
[49] M. A. Bryden, E. Zysman-Colman, *Chem. Soc. Rev.* **2021**, *50*, 7587.
[50] C. Wu, N. Corrigan, C.-H. Lim, W. Liu, G. Miyake, C. Boyer, *Chem. Rev.* **2022**, https://doi.org/10.1021/acs.chemrev.1c00409.
[51] H. Uoyama, K. Goushi, K. Shizu, H. Nomura, C. Adachi, *Nature* **2012**, *492*, 234.
[52] O. Boutureira, G. J. L. Bernardes, *Chem. Rev.* **2015**, *115*, 2174.
[53] J. H. Ko, H. D. Maynard, *Chem. Soc. Rev.* **2018**, *47*, 8998.
[54] K. M. Burridge, R. C. Page, D. Konkolewicz, *Polymer* **2020**, *211*, 123062.
[55] S. J. Bryant, C. R. Nuttelman, K. S. Anseth, *J. Biomater. Sci., Polym. Ed.* **2012**, *11*, 439.
[56] C. S. Bahney, T. J. Lujan, C. W. Hsu, M. Bottlang, J. L. West, B. Johnstone, *Eur. Cells Mater.* **2011**, *22*, 43.
[57] R. A. Olson, A. B. Korpusika, B. S. Sumerlin, *Chem. Sci.* **2020**, *11*, 5142.
[58] Q. Fu, Q. Ruan, T. G. McKenzie, A. Reyhani, J. Tang, G. G. Qiao, *Macromolecules* **2017**, *50*, 7509.
[59] J. Yeow, R. Chapman, J. Xu, C. Boyer, *Polym. Chem.* **2017**, *8*, 5012.
[60] C. Wu, K. Jung, Y. Ma, W. Liu, C. Boyer, *Nat. Commun.* **2021**, *12*, 478.
[61] C. Kerzig, X. Guo, O. S. Wenger, *J. Am. Chem. Soc.* **2019**, *141*, 2122.
[62] A. M. Mansour, K. Radacki, O. R. Shehab, *Dalton Trans.* **2021**, *50*, 10701.
[63] D. Kand, P. Liu, M. X. Navarro, L. J. Fischer, L. Rousso-Noori, D. Friedmann-Morvinski, A. H. Winter, E. W. Miller, R. Weinstain, *J. Am. Chem. Soc.* **2020**, *142*, 4970.
[64] J. Niu, D. J. Lunn, A. Pusuluri, J. I. Yoo, M. A. O'Malley, S. Mitragotri, H. T. Soh, C. J. Hawker, *Nat. Chem.* **2017**, *9*, 537.
[65] J. Geng, W. Li, Y. Zhang, N. Thottappillil, J. Clavadetscher, A. Liliana, M. Bradley, *Nat. Chem.* **2019**, *11*, 578.
[66] All rates are obtained by fitting the experimental data to the behavior derived from the rate equations for the occupation of the singlet and triplet states using the following approximations: $k_{ISC} \gg k_F, k_{nr,S}, k_{PH}, k_{RISC} \gg k_{nr,T}$.
[67] G. Ng, J. Yeow, J. Xu, C. Boyer, *Polym. Chem.* **2017**, *8*, 2841.
[68] The Stern–Volmer equation can be applied for triplet quenching in thermally activated delayed fluorescence (TADF)-type materials under the condition that $k_{RISC} \ll k_{ISC}$, which is usually valid for most TADF molecules, including the current systems, see the rates in the

Jablonski diagrams of Figure 1a and Figure S6 (Supporting Information). Details will be discussed in a forthcoming paper.
[69] C. Franco, J. OlmstedIII, *Talanta* **1990**, *37*, 905.
[70] N. J. Turro, V. Ramamurthy, J. C. Scaiano, *Principles of Molecular Photochemistry: An Introduction*, University Science Books, Sausalito, CA **2008**.
[71] P. S. Rao, E. Hayon, *J. Phys. Chem.* **1975**, *79*, 397.
[72] D. Vasudevan, H. Wendt, *J. Electroanal. Chem.* **1995**, *392*, 69.
[73] J. P. Cole, D.-F. Chen, M. Kudisch, R. M. Pearson, C.-H. Lim, G. M. Miyake, *J. Am. Chem. Soc.* **2020**, *142*, 13573.
[74] M. Hayyan, M. A. Hashim, I. M. AlNashef, *Chem. Rev.* **2016**, *116*, 3029.
[75] M. Levy, P. P. Chowdhury, P. Nagpal, *J. Biol. Eng.* **2019**, *13*, 48.
[76] J. Maillard, K. Klehs, C. Rumble, E. Vauthey, M. Heilemann, A. Fürstenberg, *Chem. Sci.* **2021**, *12*, 1352.
[77] G. E. Dobretsov, T. I. Syrejschikova, N. V. Smolina, *Biophysics* **2014**, *59*, 183.
[78] C. Boyer, V. Bulmus, J. Liu, T. P. Davis, M. H. Stenzel, C. Barner-Kowollik, *J. Am. Chem. Soc.* **2007**, *129*, 7145.
[79] W. Hou, L. Wei, L. Liu, H. Zhao, *Biomacromolecules* **2018**, *19*, 4463.
[80] T. Peters, *All About Albumin: Biochemistry, Genetics, and Medical Applications*, Academic Press, New York **1996**.
[81] J. Kim, B. Kang, S. H. Hong, *ACS Catal.* **2020**, *10*, 6013.